24

The Rate of Heat Flow through Non-Isothermal Vertical Flat Plate

T. Kranjc[1] and J. Peternelj[2]
[1]*Department of Physics and Technology, Faculty of Education, University of Ljubljana*
[2]*Faculty of Civil and Geodetic Engineering, University of Ljubljana*
Slovenia

1. Introduction

Any problem of convection consists, basically, in determining the local and/or average heat transfer coefficients connecting the local flux and/or the total transfer rate due to the relevant temperature differences. A wide variety of practical problems may be described by two-dimensional steady flow of a viscous, incompressible fluid for which a compact set of differential equations that govern the velocity and temperature fields in the fluid can be obtained. These can be solved, to a certain degree of approximation, either analytically or numerically.

Consider a flat vertical wall surrounded by air on both sides (Fig. 1). The temperature of the air far from the wall is constant on both sides and denoted by T_{0L} and T_{0R}, respectively. The problem, common in practical engineering situations, is to calculate the rate of heat flow in a stationary situation. Usually, the heat transfer between the wall and the surrounding air is characterized by the heat transfer coefficient h, defined by eqs. (1a) and (1c),

$$\dot{Q} / A = h_L (T_{0L} - T_1) , \tag{1a}$$

$$\dot{Q} / A = U (T_1 - T_2) , \tag{1b}$$

$$\dot{Q} / A = h_R (T_2 - T_{0R}) , \tag{1c}$$

where it was assumed that $T_{0L} > T_{0R}$.

As a consequence of continuity $\dot{Q} \equiv dQ / dt$ is, of course, also the heat flow through the wall with thermal transmittance U and surface area A. The temperatures of the left and right surface, T_1 and T_2, respectively, are assumed constant in the phenomenological approach based on heat transfer coefficients. It is then straightforward to show, using the above equations, that the average heat flux density through the wall is

$$\frac{\dot{Q}}{A} = \frac{T_{0L} - T_{0R}}{\frac{1}{h_L} + \frac{1}{U} + \frac{1}{h_R}} , \tag{2}$$

In what follows we will employ the laminar boundary-layer theory and free convection equations (Grimson, 1971; Landau & Lifshitz, 1987) in order to determine the surface temperatures T_1 and T_2 and the heat transfer coefficients in such a way that eqs. (1) and (2) describe correctly the total heat flow $\dot{Q}$ across the wall.

Free convection along a vertical flat plate has been studied extensively in the past, however, it has been commonly restricted to one surface of the wall only (Pohlhausen, 1921; Ostrach, 1953; Miyamoto et al., 1980; Pozzi & Lupo, 1988; Vynnycky & Kimura, 1996; Pop & Ingham, 2001). The thermal conditions at the other surface have been prescribed by either constant temperature or constant heat flux. In the situation discussed in this chapter only the temperature of the fluid far away from the wall is prescribed.

2. Free convection equations for a flat vertical wall

To analyze free convection on the right surface where the convective flow is upward, we choose the origin of the coordinate system at the lower edge of the right surface of the wall (Fig. 1).

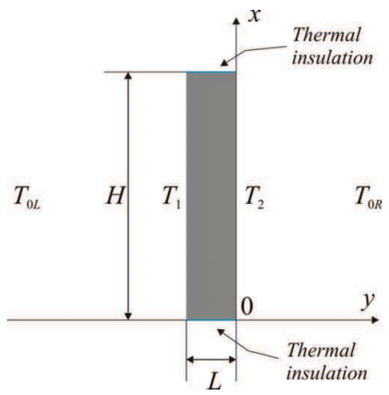

Fig. 1. Free convection at a flat vertical surface.

The x-axis is vertical and the y-axis perpendicular to the wall of height H and width L. Within the framework of the boundary-layer theory the equations of free convection valid for $y > 0$ are (Landau & Lifshitz, 1987):

$$u(\partial u/\partial x) + v(\partial u/\partial y) = \nu(\partial^2 u/\partial y^2) + \beta g(T - T_{0R}), \tag{3a}$$

$$u(\partial T/\partial x) + v(\partial T/\partial y) = a(\partial^2 T/\partial y^2), \tag{3b}$$

$$\partial u/\partial x + \partial v/\partial y = 0, \tag{3c}$$

subject to the boundary conditions

$$u(x, 0) = v(x, 0) = 0, \tag{4a}$$

$$u(x, \infty) = 0,\ T(x, \infty) = T_{0R}. \tag{4b}$$

u and v are the x- and y-component of the velocity field, g is the acceleration of gravity, β is the thermal-expansion coefficient of the air, $a = k\rho/c_p$ its thermal diffusivity, and $\nu = \eta/\rho$ the kinematic viscosity.

To satisfy eq. (3c) we introduce the stream function $\psi(x, y)$ such that $u = \partial\psi/\partial y$ and $v = -\partial\psi/\partial x$. Similarity arguments (Landau & Lifshitz, 1987) for free convection suggest that we write the stream function as $\psi(x, y) = \nu\, \psi^*(x/H, y/H, G, P)$, where $G = \beta g(T_s - T_{0R})H^3/\nu^2$ and $P = \nu/a$ are the Grashof and Prandtl numbers, respectively, and T_s is a temperature characteristic of the surface. In addition, since we anticipate the surface temperatures to be close to uniform, except in the vicinity of $x = 0$ (Miyamoto et al., 1980; Pozzi & Lupo, 1988; Vynnycky & Kimura, 1996), we further specify the stream function to have the form ($y > 0$)

$$\psi_R(x, y) = \nu_R G_R^{1/4} (4x^*)^{3/4} [\Phi_R(\xi) + \phi_R(x^*, \xi)], \tag{5}$$

where $x^* = x/H$, $y^* = y/H$, $\xi = G_R^{1/4} y^*/(4x^*)^{1/4}$ and $G_R = \beta_R g(T_2 - T_{0R})H^3/\nu_R^2$. $\Phi_R(\xi)$ represents the Pohlhausen solution (Grimson, 1971; Landau & Lifshitz, 1987; Pohlhausen, 1921) describing free convection on the flat vertical wall with uniform temperature $T_2 > T_{0R}$. The temperature distribution in the air to the right of the wall is written correspondingly as

$$T_R(x, y) = T_{0R} + (T_2 - T_{0R}) [\Theta_R(\xi) + \theta_R(x^*, \xi)], \tag{6}$$

where $\Theta_R(\xi)$ is the Pohlhausen temperature function associated with $\Phi_R(\xi)$. These two functions are obtained as solutions of (see Landau & Lifshitz, 1987)

$$\Phi_R''' + 3\Phi_R \Phi_R'' - 2\Phi_R'^2 + \Theta_R = 0, \tag{7a}$$

$$\Theta_R'' + 3P_R \Phi_R \Theta_R' = 0, \tag{7b}$$

satisfying the boundary conditions

$$\Phi_R(0) = \Phi_R'(0) = \Phi_R'(\infty) = 0, \quad \Theta_R(0) = 1, \Theta_R(\infty) = 0, \tag{7c}$$

and the primes denote differentiation with respect to ξ. $\phi_R(x^*, \xi)$ and $\theta_R(x^*, \xi)$ are, presumably, small corrections due to the fact that the surface temperatures are not exactly uniform.

As pointed out in Ostrach (1953), the choice of the variable ξ defined above essentially implies that the conditions imposed on the velocities and temperature at $y = \infty$ (or $\xi = \infty$) should also be satisfied, for $y \neq 0$, at $x = 0$. This seems reasonable physically if it is understood as a statement that on the right-hand side the convective flow starts at the bottom edge of the wall. Considering the boundary conditions (4b) and (7c) referring to temperature, it follows from (6) that $T_R(x \neq 0, y = 0) = T_2 + (T_2 - T_{0R})\, \theta_R(x \neq 0, \xi = 0)$ and $T_R(x = 0, y \neq 0) = T_{0R}$. In the vicinity of $x = y = 0$, the boundary layer approximation breaks down and the calculation based on this approximation cannot yield reliable results as pointed out already by Miyamoto et al. (1980). However, we believe that this conclusion is not so crucial since the contribution of the surface area near the leading edge of the convective flow to the total heat rate is proportional to x_0/H, where x_0 is small compared to H (Pozzi & Lupo, 1988).

To describe free convection on the left surface of the wall we must reverse the coordinate axes since there the local buoyancy force is directed vertically downward. Thus we choose the origin of the coordinate system at the upper edge of the left surface, the x-axis is oriented vertically downward and the y-axis is perpendicular to the wall and oriented to the left (Fig. 2, left).

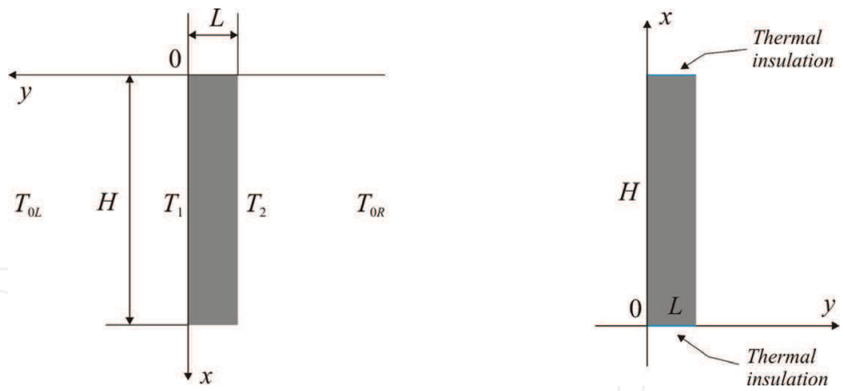

Fig. 2. Left: Coordinate system for convection to the left of the wall. Right: Coordinate system for temperature distribution within the wall.

We write as above,

$$\psi_L(x, y) = \nu_L G_L^{1/4}(4x^*)^{3/4}\,[\Phi_L(\xi) + \phi_L(x^*, \xi)], \tag{8}$$

$$T_L(x, y) = T_{0L} + (T_1 - T_{0L})\,[\Theta_L(\xi) + \theta_L(x^*, \xi)], \tag{9}$$

where $G_L = \beta_L(-g)(T_1 - T_{0L})H^3/\nu_L^2$, $\xi = G_L^{1/4}y^*/(4x^*)^{1/4}$ and $\Phi_L(\xi)$ and $\Theta_L(\xi)$ satisfy identical equations as Φ_R and Θ_R, provided that we replace $g \to -g$ in eq. (3a) and use the parameters characteristic for the air to the left of the wall.

3. Temperature distribution inside the wall

The steady state temperature distribution within the wall satisfies Laplace's equation,

$$\frac{\partial^2 T}{\partial x^2} + \frac{\partial^2 T}{\partial y^2} = 0\,. \tag{10}$$

At the bottom and upper side the wall is assumed to be insulated and consequently the boundary conditions, $\partial T/\partial x\,|_{x=0} = \partial T/\partial x\,|_{x=H} = 0$, are imposed (Vynnycky & Kimura, 1996). We choose the origin of the coordinate system, used for the wall only, at the lower edge of the left surface of the wall (Fig. 2, right). With the x-axis vertical and the y-axis perpendicular to the wall, we can write the temperature distribution within the wall as

$$T(x,y) = T_1 + \frac{y}{L}(T_2 - T_1) + \sum_{n=1}^{\infty}\left[\left(T_1 - T_{0L}\right)A_n \sinh\left(\tfrac{n\pi(L-y)}{H}\right) + \left(T_2 - T_{0R}\right)B_n \sinh\left(\tfrac{n\pi y}{H}\right)\right]\cos\left(\tfrac{n\pi x}{H}\right). \tag{11}$$

The average wall surface temperatures $T_1 = \frac{1}{H}\int_0^H T(x,0)dx$, $T_2 = \frac{1}{H}\int_0^H T(x,L)dx$, ($T_1 > T_2$) and the coefficients A_n and B_n are determined by requiring that the temperatures of the two media must be equal at the respective boundaries and, moreover, the heat flux out of one medium must equal the heat flux into the other medium at each of the two boundaries.
Taking into account the relative displacement and orientation of the various coordinate systems, this yields

$$\theta_L(x^*,0)=\sum_{n=1}^{\infty}A_n\sinh\frac{n\pi L}{H}\cos n\pi(1-x^*)=\sum_{n=1}^{\infty}(-1)^n A_n\sinh\frac{n\pi L}{H}\cos n\pi x^*, \tag{12a}$$

$$\theta_R(x^*,0)=\sum_{n=1}^{\infty}B_n\sinh\frac{n\pi L}{H}\cos n\pi x^*, \tag{12b}$$

and

$$-k_L\left(\frac{T_1-T_{0L}}{H}\right)\left[\left(\frac{G_L}{4x^*}\right)^{1/4}\left(\Theta'_L(0)+\theta'_L(x^*,0)\right)\right]= \tag{13a}$$
$$U(T_2-T_1)+\sum_{n=1}^{\infty}(-1)^n\left\{U(T_{0L}-T_1)A_n\frac{n\pi L}{H}\cosh\frac{n\pi L}{H}+U(T_2-T_{0R})B_n\frac{n\pi L}{H}\right\}\cos n\pi x^*,$$

$$k_R\left(\frac{T_2-T_{0R}}{H}\right)\left[\left(\frac{G_R}{(4x^*)}\right)^{1/4}\left(\Theta'_R(0)+\theta'_R(x^*,0)\right)\right]= \tag{13b}$$
$$U(T_2-T_1)+\sum_{n=1}^{\infty}\left\{U(T_{0L}-T_1)A_n\frac{n\pi L}{H}+U(T_2-T_{0R})B_n\frac{n\pi L}{H}\cosh\frac{n\pi L}{H}\right\}\cos n\pi x^*,$$

where a uniform composition of the wall was assumed, $U = k_w/L$, and $k_{L,R}$ are thermal conductivities of the air at the left and right surface of the wall, respectively.
As already stressed, we are interested in the total rate of heat flow through the wall. Integrating eqs. (13) with respect to x^* we obtain

$$-k_L\left(\frac{T_{0L}-T_1}{H}\right)\left[\left(\frac{G_L}{4}\right)^{1/4}\left(\frac{4}{3}\Theta'_L(0)+\int_0^1(x^*)^{\frac{3}{4}-1}\theta'_L(x^*,0)dx^*\right)\right]=U(T_1-T_2), \tag{14a}$$

$$-k_R\left(\frac{T_2-T_{0R}}{H}\right)\left[\left(\frac{G_R}{4}\right)^{1/4}\left(\frac{4}{3}\Theta'_R(0)+\int_0^1(x^*)^{\frac{3}{4}-1}\theta'_R(x^*,0)dx^*\right)\right]=U(T_1-T_2). \tag{14b}$$

Using the definition of the Grashof number and the relations $\beta_{L,R}\approx 1/T_{0L,R}$, we can rewrite eqs. (14) in the form

$$T_{0L}-T_1=(T_2-T_{0R})\left(\gamma^4\frac{T_{0L}}{T_{0R}}\right)^{1/5}, \tag{15a}$$

$$-\frac{\kappa_R}{\sqrt{2}}\left(\frac{gH^3}{\nu_R^2}\right)^{\frac{1}{4}}\left(\tfrac{4}{3}\Theta'_R(0)+J_R\right)\left(\frac{T_2-T_{0R}}{T_{0R}}\right)^{\frac{5}{4}}+\left(1+\left(\gamma^4\frac{T_{0L}}{T_{0R}}\right)^{\frac{1}{5}}\right)\left(\frac{T_2-T_{0R}}{T_{0R}}\right)-\left(\frac{T_{0L}-T_{0R}}{T_{0R}}\right)=0, \tag{15b}$$

where

$$\gamma=\left(\frac{\nu_L}{\nu_R}\right)^{1/2}\left(\frac{k_R}{k_L}\right)\frac{\frac{4}{3}\Theta'_R(0)+J_R}{\frac{4}{3}\Theta'_L(0)+J_L}, \tag{15c}$$

$$J_{L,R} = \int_0^1 (x^*)^{-\frac{1}{4}} \theta'_{L,R}(x^*,0) dx^* , \tag{15d}$$

and

$$\kappa_{L,R} = \frac{k_{L,R} L}{k_w H} . \tag{15e}$$

The total rate of heat flow per unit area of the wall $q \equiv \dot{Q} / A$ is, referring to eqs. (14), equal to $U(T_1 - T_2)$. To proceed, we use eqs. (1a, c), (2) and (15a) to determine the heat transfer coefficients. From (1a, c) and (15a) it follows

$$\frac{h_R}{h_L} = \left(\gamma^4 \frac{T_{0L}}{T_{0R}} \right)^{1/5} \tag{16}$$

and, equating (2) and (1c), we obtain

$$h_R = \bar{N}u^{(R)} \frac{k_R}{H} . \tag{17a}$$

Here,

$$\bar{N}u^{(R)} = \frac{1}{\kappa_R} \left\{ \frac{T_{0L} - T_{0R}}{T_2 - T_{0R}} - \left[1 + \left(\gamma^4 \frac{T_{0L}}{T_{0R}} \right)^{1/5} \right] \right\} \tag{17b}$$

is the average Nusselt number, associated with the right-hand surface of the wall. (Of course, h_R as written in (17a) is also the average heat transfer coefficient, but we shall omit the bar above the symbol.) Writing similarly $h_L = \bar{N}u^{(L)} \frac{k_L}{H}$ and using eqs. (16, 17a), we obtain the corresponding expression for $\bar{N}u^{(L)}$,

$$\bar{N}u^{(L)} = \frac{k_R}{k_L} \left(\gamma^4 \frac{T_{0L}}{T_{0R}} \right)^{-1/5} \qquad \bar{N}u^{(R)} = \frac{1}{\kappa_L} \left\{ \frac{T_{0L} - T_{0R}}{T_{0L} - T_1} - \left[1 + \left(\gamma^4 \frac{T_{0L}}{T_{0R}} \right)^{-1/5} \right] \right\} . \tag{17c}$$

Furthermore, the solution of eq. (15b) can be calculated by Newton's method of successive approximations with the initial approximate solution chosen as

$$\left(\frac{T_2 - T_{0R}}{T_{0R}} \right)_0 = \frac{\left(\frac{T_{0L} - T_{0R}}{T_{0R}} \right)}{1 + \gamma^{4/5} \left(\frac{T_{0L}}{T_{0R}} \right)^{1/5} - \frac{1}{\sqrt{2}} \kappa_R \left(\frac{gH^3}{\nu_R^2} \right)^{1/4} \left(\frac{4}{3} \Theta'_R(0) + J_R \right) \left(\frac{T_{0L} - T_{0R}}{T_{0R}} \right)^{1/4}} , \tag{18}$$

obtained from (15b) by writing

$$\left(\frac{T_2 - T_{0R}}{T_{0R}}\right)^{5/4} \cong \left(\frac{T_2 - T_{0R}}{T_{0R}}\right)\left(\frac{T_{0L} - T_{0R}}{T_{0R}}\right)^{1/4}.$$

In the lowest approximation, (17b) and (17c) then become

$$\bar{N}u^{(R)} = -\frac{1}{\sqrt{2}}\left(\frac{gH^3}{{\nu_R}^2}\right)^{1/4}\left(\frac{4}{3}\Theta_R'(0) + J_R\right)\left(\frac{T_{0L} - T_{0R}}{T_{0R}}\right)^{1/4}, \tag{19a}$$

$$\bar{N}u^{(L)} = \left(\gamma^4 \frac{T_{0L}}{T_{0R}}\right)^{1/20}\left\{-\frac{1}{\sqrt{2}}\left(\frac{gH^3}{\nu_L^2}\right)^{1/4}\left(\frac{4}{3}\Theta_L'(0) + J_L\right)\left(\frac{T_{0L} - T_{0R}}{T_{0L}}\right)^{1/4}\right\}. \tag{19b}$$

The average heat flux density $\dot{Q}/A$ can be now calculated easily by using eq. (2), for example, and the expressions for the heat transfer coefficients as determined above.
Using the result obtained by Kao et al. (1977) and quoted by Miyamoto et al. (1980) (eq. (13)), we can calculate $\frac{4}{3}\Theta_R'(0) + J_R$. The heat flux density at the right surface of the wall (the analysis for the left surface is identical)

$$q(x^*) = -k_R\left(\frac{T_2 - T_{0R}}{H}\right)\left(\frac{G_R}{4x^*}\right)^{1/4}\left(\Theta_R'(0) + \theta_R'(x^*,0)\right) \tag{20a}$$

may be, according to Miyamoto et al. (1980), for $P = 0.7$, approximated closely by

$$q(x^*) = k_R\left(\frac{T_2 - T_{0R}}{H}\right)\left(\frac{G_R}{4}\right)^{1/4}\left(c_1\frac{F_R^{3/2}}{\varsigma_R^{1/4}} + c_2\frac{\varsigma_R^{3/4}}{F_R^{1/2}}\frac{dF_R}{dx^*}\right), \tag{20b}$$

where $c_1 = 0.4995$, $c_2 = 0.2710$ and

$$\begin{aligned} F_R(x^*) &= \frac{T_R(x,0) - T_{0R}}{T_2 - T_{0R}} = 1 + \theta_R(x^*,0), \\ \varsigma_R(x^*) &= \int_0^{x^*} F_R dx^*. \end{aligned} \tag{20c}$$

Equating the right-hand sides of (20a, b) and integrating the resulting equation with respect to x^* from 0 to 1, we obtain

$$\tfrac{4}{3}\Theta_{L,R}'(0) + J_{L,R} = -2c_2F_{L,R}^{1/2}(1) - \left(c_1 - \tfrac{3}{2}c_2\right)\int_0^1 dx^*\frac{F_{L,R}^{3/2}}{\varsigma_{L,R}^{1/4}}. \tag{21}$$

4. Equations determining $F_{L,R}(x^*)$

In order to calculate (21), we rewrite the boundary conditions (13), using eqs. (12), (14), (15), (20) and (21), as follows:

$$-\kappa_L\left(\frac{G_L}{4}\right)^{1/4}\left[c_1\frac{F_L^{3/2}}{\varsigma_L^{1/4}}+c_2\frac{\varsigma_L^{3/4}}{F_L^{1/2}}\frac{dF_L}{dx^*}\right]=-\kappa_L\left(\frac{G_L}{4}\right)^{1/4}\left[2c_2F_L^{1/2}(1)+(c_1-\tfrac{3}{2}c_2)\int_0^1 dx^*\frac{F_L^{3/2}}{\varsigma_L^{1/4}}\right]+$$
$$2\sum_{n=1}^{\infty}\left\{\frac{n\pi L}{H}\coth\frac{n\pi L}{H}\int_0^1 dx^*F_L\cos n\pi x^*+(-1)^n\left(\gamma^4\frac{T_{0L}}{T_{0R}}\right)^{-1/5}\frac{\frac{n\pi L}{H}}{\sinh\frac{n\pi L}{H}}\int_0^1 dx^*F_R\cos n\pi x^*\right\}\cos n\pi x^*, \tag{22a}$$

$$-\kappa_R\left(\frac{G_R}{4}\right)^{1/4}\left[c_1\frac{F_R^{3/2}}{\varsigma_R^{1/4}}+c_2\frac{\varsigma_R^{3/4}}{F_R^{1/4}}\frac{dF_R}{dx^*}\right]=-\kappa_R\left(\frac{G_R}{4}\right)^{1/4}\left[2c_2F_R^{1/2}(1)+(c_1-\tfrac{3}{2}c_2)\int_0^1 dx^*\frac{F_R^{3/2}}{\varsigma_R^{1/4}}\right]+$$
$$2\sum_{n=1}^{\infty}\left\{(-1)^n\left(\gamma^4\frac{T_{0L}}{T_{0R}}\right)^{1/5}\frac{\frac{n\pi L}{H}}{\sinh\frac{n\pi L}{H}}\int_0^1 dx^*F_L\cos n\pi x^*+\frac{n\pi L}{H}\coth\frac{n\pi L}{H}\int_0^1 dx^*F_R\cos n\pi x^*\right\}\cos n\pi x^*. \tag{22b}$$

If we multiply both sides of eqs. (22) by cos($n\pi x^*$), integrate with respect to x^* from 0 to 1 and rearrange the terms, we obtain

$$\int_0^1 F_L\cos n\pi x^*dx^*=-\kappa_L\left(\frac{G_L}{4}\right)^{1/4}\left[\int_0^1 dx^*\left(c_1\frac{F_L^{3/2}}{\varsigma_L^{1/4}}+c_2\frac{\varsigma_L^{3/4}}{F_L^{1/2}}\frac{dF_L}{dx^*}\right)\cos n\pi x^*\right]\frac{\coth(n\pi L/H)}{(n\pi L/H)}$$
$$+(-1)^n\kappa_R\left(\gamma^4\frac{T_{0L}}{T_{0R}}\right)^{-1/5}\left(\frac{G_R}{4}\right)^{1/4}\left[\int_0^1 dx^*\left(c_1\frac{F_R^{3/2}}{\varsigma_R^{1/4}}+c_2\frac{\varsigma_R^{3/4}}{F_R^{1/2}}\frac{dF_R}{dx^*}\right)\cos n\pi x^*\right]\frac{1}{\frac{n\pi L}{H}\sinh\frac{n\pi L}{H}}, \tag{23a}$$

$$\int_0^1 F_R\cos n\pi x^*dx^*=(-1)^n\kappa_L\left(\gamma^4\frac{T_{0L}}{T_{0R}}\right)^{1/5}\left(\frac{G_L}{4}\right)^{1/4}\left[\int_0^1 dx^*\left(c_1\frac{F_L^{3/2}}{\varsigma_L^{1/4}}+c_2\frac{\varsigma_L^{3/4}}{F_L^{1/2}}\frac{dF_L}{dx^*}\right)\cos n\pi x^*\right]\times$$
$$\frac{1}{\frac{n\pi L}{H}\sinh\frac{n\pi L}{H}}-\kappa_R\left(\frac{G_R}{4}\right)^{1/4}\left[\int_0^1 dx^*\left(c_1\frac{F_R^{3/2}}{\varsigma_R^{1/4}}+c_2\frac{\varsigma_R^{3/4}}{F_R^{1/2}}\frac{dF_R}{dx^*}\right)\cos n\pi x^*\right]\frac{\coth(n\pi L/H)}{n\pi L/H)}. \tag{23b}$$

5. Numerical results

We will attempt to solve eqs. (23) by approximating $F_{L,R}(x^*) - 1 = \theta_{L,R}(x^*, 0) \equiv \theta_{L,R}(x^*)$ by a polynomial,

$$\theta_{L,R}(x^*)=-a_{L,R}^{(0)}+a_{L,R}^{(1)}x^*+a_{L,R}^{(2)}x^{*2}+a_{L,R}^{(3)}x^{*3}+a_{L,R}^{(4)}x^{*4}+\cdots, \tag{24}$$

where, as a consequence of eqs. (12),

$$0=-a_{L,R}^{(0)}+\left(\tfrac{1}{2}a_{L,R}^{(1)}+\tfrac{1}{3}a_{L,R}^{(2)}+\tfrac{1}{4}a_{L,R}^{(3)}+\tfrac{1}{5}a_{L,R}^{(4)}+\cdots\right). \tag{25}$$

The natural approach to solving for coefficients $a_{L,R}^{(i)}$, i = 1, 2, 3, ... in eq. (24) is using the Newton method. However, we also employed the iteration method as proposed by Miyamoto et al. (1980). It turned out that the applicability of the simpler iteration procedure is limited to a restricted range of parameters appearing in Eqs. (23) ($G_{L,R}$, $\kappa_{L,R}$, $T_{0R,L}$, γ and

aspect ratio L/H). It works well for plates with small aspect ratio and high conductivity (k_w), like stainless steel or aluminum. But it breaks down for walls with large aspect ratio and with the conductivity coefficient 10–100 times lower (such as the thermal conductivity of brick, for example), and a better calculational method has to be applied. This is described in the Mathematical note, Section 7.

The knowledge of $F_{L,R}(x^*)$ makes it possible to calculate the temperatures T_1 and T_2 at the wall surfaces as well as the heat flux (or the heat flux density) through the wall, $\dot{Q}$ (or $\dot{Q}/A$). Using eqs. (17b, c), we can express the temperatures T_1 and T_2 at the wall surfaces in terms of the Nusselt numbers,

$$T_1 = T_{0L} - \frac{T_{0L} - T_{0R}}{\kappa_L \bar{N}u^{(L)} + 1 + [\gamma^4 (T_{0L}/T_{0R})]^{-1/5}}, \tag{26a}$$

$$T_2 = T_{0R} + \frac{T_{0L} - T_{0R}}{\kappa_R \bar{N}u^{(R)} + 1 + [\gamma^4 (T_{0L}/T_{0R})]^{1/5}}. \tag{26b}$$

Subtracting the above two equations, we obtain the temperature difference across the wall,

$$T_1 - T_2 =$$

$$(T_{0L} - T_{0R}) \left[1 - \left(\frac{1}{\kappa_R \bar{N}u^{(R)} + 1 + [\gamma^4 (T_{0L}/T_{0R})]^{1/5}} + \frac{1}{\kappa_L \bar{N}u^{(L)} + 1 + [\gamma^4 (T_{0L}/T_{0R})]^{-1/5}} \right) \right]. \tag{27}$$

The Nusselt numbers $\bar{N}u^{(R)}$ and $\bar{N}u^{(L)}$ are given in the lowest approximation by eqs. (19a, b). From (27) and (1b), the average flux density through the wall (equal to the average heat flux density through the air layers at the wall) can be written:

$$\frac{\dot{Q}}{A} = U(T_{0L} - T_{0R}) \left[1 - \left(\frac{1}{\kappa_R \bar{N}u^{(R)} + 1 + [\gamma^4 (T_{0L}/T_{0R})]^{\frac{1}{5}}} + \frac{1}{\kappa_L \bar{N}u^{(L)} + 1 + [\gamma^4 (T_{0L}/T_{0R})]^{-\frac{1}{5}}} \right) \right]. \tag{28}$$

Finally, through the eq. (17a), the heat transfer (convection) coefficients can be expressed in terms of the Nusselt numbers as

$$h_{R,L} = \left(\frac{k_{R,L}}{H} \right) \bar{N}u^{(R,L)}. \tag{29}$$

We performed numerical calculations for stainless steel and aluminum plates (compare Miyamoto et al. (1980)), as well as for walls of various dimensions and thermal conductivities comparable to brick or concrete, surrounded by air. We present some of the results for the air temperatures T_{0L} = 30 °C = 303 K and T_{0R} = 20 °C = 293 K.

5.1 Stainless steel plate

Thermal conductivities for air and steel are $k_{L,R} = k_a = 2.63 \times 10^{-2}$ W/mK (air at ~300 K) and k_w = 16 W/m · K, respectively. For a plate 1 cm thick and 40 cm high (aspect ratio L/H = 0.025), $\kappa_L = \kappa_R = \kappa = (k_a/k_w)(L/H) = 4.1 \times 10^{-5}$, and for the temperature difference $T_{0L} - T_1 \cong$

$T_2 - T_{0R} \cong 5.0$ K, the Grashof number takes the value $G_L \approx G_R \approx G = 4.2 \times 10^7$. The coefficient γ (Eq. (15c)) is very close to 1. The function $\theta_L(x^*)$ is shown in Fig. 3.
With the results for $F_{L,R}(x^*)$ and using $\Theta'_{L,R}(0) = -0.4995$ (for the Prandtl number $P = 0.70$), we get $J_L \cong J_R = -0.0041$ and, consequently, using equation (19),

$$\bar{N}u^{(R)} = 0.474\left(\frac{gH^3}{\nu_R^2}\right)^{1/4}\left(\frac{T_{0L}-T_{0R}}{T_{0R}}\right)^{1/4} \tag{30a}$$

and

$$\bar{N}u^{(L)} = \left(\frac{T_{0R}}{T_{0L}}\right)^{1/5}\bar{N}u^{(R)} = 0.474\left(\frac{T_{0L}}{T_{0R}}\right)^{1/20}\left(\frac{gH^3}{\nu_L^2}\right)^{1/4}\left(\frac{T_{0L}-T_{0R}}{T_{0L}}\right)^{1/4}. \tag{30b}$$

In the present case, the value of the Nusselt number is $\bar{N}u^{(R)} = \bar{N}u^{(L)} = 45$. The temperature drop across the plate is negligible ($T_1 - T_2 \sim 10^{-2}$ K), being only a tiny fraction (~10^{-3}) of the air temperature difference on the two sides of the plate. Essentially the whole temperature drop takes place within the boundary layers at the plate surfaces.

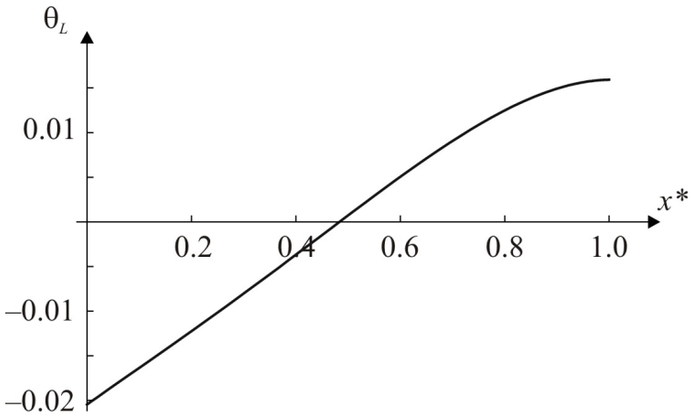

Fig. 3. Stainless steel. Correction $\theta_L(x^*)$ to the Pohlhausen solution for a steel plate (L/H = 0.05, $G_L \approx G_R = 4.2 \times 10^7$, $\kappa_L = \kappa_R = 4.1 \times 10^{-5}$, and $T_{0L} = 30$ °C, $T_{0R} = 20$ °C). The correction $\theta_R(x^*)$ differs only insignificantly from $\theta_L(x^*)$.

The heat flux density is equal to ~15 W/m², and the heat transfer coefficients are ~3 W/(m² ·K).
If the aspect ratio increases at constant height, the Grashof number increases, while $\theta_{L,R}(x^*)$ decrease. If the height increases at constant aspect ratio, the Grashof number as well as $\theta_{L,R}(x^*)$ increase.

5.2 Aluminum plate

The thermal conductivity of aluminum is k_w = 203 W/m ·K. If the plate has the same dimensions as the steel plate (1 cm thick, 40 cm high, aspect ratio L/H = 0.025), $\kappa_L = \kappa_R = \kappa = (k_a/k_w)(L/H) = 3.24 \times 10^{-6}$, and for the temperature difference of 5.0 K, the Grashof number takes the value $G_L \approx G_R \approx G = 4.2 \times 10^7$. Again, $\gamma \cong 1$. The function $\theta_L(x^*)$ is shown in Fig. 4. In this case, we obtain (P = 0.70) $J_L \cong J_R = -0.0035$ and the Nusselt number is

$$\bar{N}u^{(R)} = 0.473\left(\frac{gH^3}{\nu_R^2}\right)^{1/4}\left(\frac{T_{0L}-T_{0R}}{T_{0R}}\right)^{1/4}. \tag{31}$$

In the case of aluminum, the value of the Nusselt number is again $\bar{N}u^{(R)} = \bar{N}u^{(L)} = 45$. The temperature drop across the plate is negligible: $T_1 - T_2 \sim 10^{-3}$ K, $(T_1 - T_2)/(T_{0L} - T_{0L}) \sim 10^{-4}$; again almost all of the temperature drop occurs within the boundary layers at the plate surfaces.

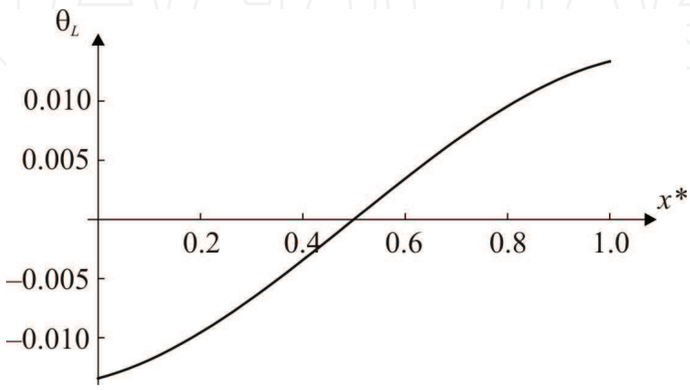

Fig. 4. Aluminum. Correction $\theta_L(x^*)$ to the Pohlhausen solution for an aluminum plate ($L/H = 0.05$, $G_L \approx G_R = 4.2 \times 10^7$, $\kappa_L = \kappa_R = 3.24 \times 10^{-6}$, and $T_{0L} = 30\ ^oC$, $T_{0R} = 20\ ^oC$). The correction $\theta_R(x^*)$ differs insignificantly from $\theta_L(x^*)$.

The heat flux density and the heat transfer coefficients are approximately the same as in the previous case, namely 15 W/m^2 and ~3 W/m^2 · K, respectively.

5.3 Brick wall

Next we consider a 10 cm thick and 200 cm high wall (aspect ratio $L/H = 0.05$) with thermal conductivity $k_w = 0.72$ W/m · K (brick) and surrounded by air; for the temperature difference of 4.3 K, the Grashof numbers take the values $G_L = 4.55 \times 10^9$ and $G_R = 4.52 \times 10^9$, respectively, and $\kappa_L = \kappa_R = \kappa = (k_a/k_w)(L/H) = 0.00183$. The coefficient $\gamma \approx 1$.

While in the previous cases, the iteration method (Miyamoto et al., 1980) was sufficient to solve Eqs. (23), in this example only the Newton method is applicable. The function $\theta_L(x^*)$ ($\theta_R(x^*)$ being essentially identical) is shown in Fig. 5. Here the temperature drop across the wall is $0.13(T_{0L} - T_{0R})$; $J_R = -0.0570$ and $J_L = -0.0565$ resulting in

$$\bar{N}u^{(R)} = 0.511\left(\frac{gH^3}{\nu_R^2}\right)^{1/4}\left(\frac{T_{0L}-T_{0R}}{T_{0R}}\right)^{1/4}, \tag{32}$$

and $\bar{N}u^{(L)}$ is given by a similar expression.

In this case, the value of the Nusselt number is $\bar{N}u^{(R)} \cong \bar{N}u^{(L)} \cong 163$. The temperature drop across the plate is $T_1 - T_2 = 1.3$ K. The heat flux density is approximately 9 W/m^2, and the heat transfer coefficients ~2 W/(m^2 · K).

If the aspect ratio increases at constant height, the Grashof number increases, while $\theta_{L,R}(x^*)$ decrease. If the height increases at constant aspect ratio, the Grashof number as well as $\theta_{L,R}(x^*)$ increase.

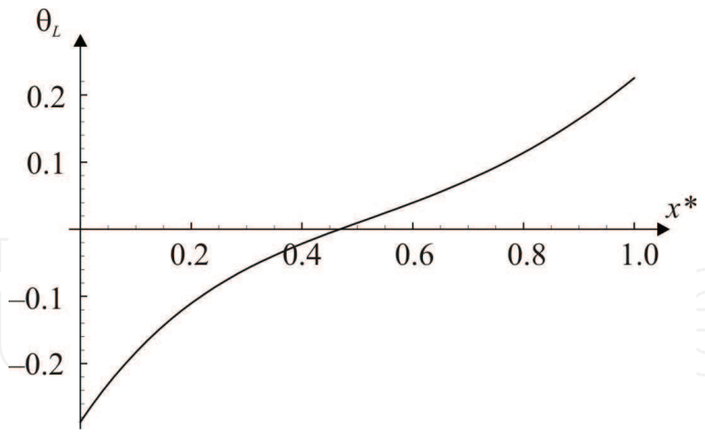

Fig. 5. Brick. The correction $\theta_L(x^*)$ to the Pohlhausen solution for a wall with k_w = 0.72 W/m ·K (L/H = 0.05, $G_L \approx G_R \approx 4.5 \times 10^9$, $\kappa_L = \kappa_R =$ 0.00183, and T_{0L} = 30 °C, T_{0R} = 20 °C).

5.4 Concrete wall

Finally, we consider a concrete (stone mix) wall, again 10 cm thick and 2 m high (aspect ratio L/H = 0.05) with thermal conductivity k_w = 1.4 W/m ·K and surrounded by air. For the temperature difference of 4.7 K, the Grashof numbers are $G_L = 4.84 \times 10^9$ and $G_R = 4.97 \times 10^9$, respectively, and $\kappa_L = \kappa_R = \kappa = (k_a/k_w)(L/H) = 0.00094$. The coefficient $\gamma = 1.0005 \approx 1$.

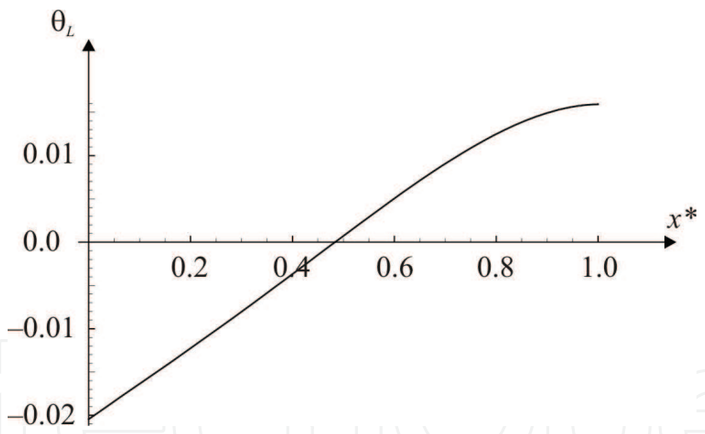

Fig. 6. Concrete (mix stone). The correction $\theta_L(x^*)$ to the Pohlhausen solution for a wall with k_w = 1.4 W/m ·K (L/H = 0.05, $G_L = 4.84 \times 10^9$, $G_R = 4.97 \times 10^9$, $\kappa_L = \kappa_R =$ 0.00094, and T_{0L} = 30 °C, T_{0R} = 20 °C).

The function $\theta_L(x^*)$ (or $\theta_R(x^*)$) is shown in Fig. 6. Here the temperature drop across the wall is $0.07(T_{0L} - T_{0R})$; J_R = –0.0558 and J_L = –0.0555 resulting in

$$\bar{N}u^{(R)} = 0.507\left(\frac{gH^3}{\nu_R^2}\right)^{1/4}\left(\frac{T_{0L}-T_{0R}}{T_{0R}}\right)^{1/4}. \tag{33}$$

In this case, the Nusselt numbers are $\bar{N}u^{(R)} \cong \bar{N}u^{(L)} \cong 163$. The temperature drop across the plate is $T_1 - T_2$ = 0.7 K.

The heat flux density is approximately 10 W/m², and the heat transfer coefficients ~2 W/m² ·K.

6. Conclusion

Free convection along both sides of a vertical flat wall was considered within the framework of the laminar boundary-layer theory and for the case where only the temperatures of the fluid far away from the wall are known. It has been shown how to determine the average surface temperatures T_1 and T_2 together with the corresponding heat transfer coefficients in order for the equations (1) and (2) to yield the correct value for the total heat flow across the wall. In particular, if the small surface temperature variations $\theta_{L,R}(x^*)$ are neglected, the heat transfer from the wall to the fluid or vice versa is determined by the Pohlhausen solutions $\Theta_{L,R}(\xi)$ only. The corresponding Nusselt number $\bar{N}u^{(R)}$, for example, is obtained from (19a) by neglecting the J_R term. This yields

$$\bar{N}u^{(R)} = 0.471\left(\frac{gH^3}{\nu_R^2}\right)^{1/4}\left(\frac{T_{0L}-T_{0R}}{T_{0R}}\right)^{1/4}. \tag{34}$$

It differs less that one percent as compared to the values given by eqs. (30a) and (31) which are valid for good thermal conductors. Consequently, the Pohlhausen solution can be therefore safely used in this case. For poor thermal conductors, like brick or concrete walls, the corrections may be more substantial. In particular, for a brick wall, the correction, obtained by comparing (32) and (34), is roughly 10 percent and it should be taken into account.

In numerical calculations, the Newton method turned out to be sufficient in solving the equations for the temperature corrections to the Pohlhausen solution. The simple iteration procedure, however, was found to have a rather restricted range of validity (large thermal conductivity, large aspect ratio of the plate).

7. Mathematical note

The system of equations (23a) and (23b) is defined for n = 1, 2,… only. For n = 0, the equations of both parts of the system simplify to a normalization conditions,

$$\int_0^1 F_L(x^*)dx^* = 1\,, \quad \int_0^1 F_R(x^*)dx^* = 1\,. \tag{MN.1}$$

It is natural to look for the functions F_L and F_R as elements of some linear subspace $S_m \subset C^r([0, 1])$ where S_m should become dense in $C^r([0, 1])$ as $m \to \infty$. Let us denote the basis of S_m as

$$s_i, \quad i = 0,1,\ldots, m.$$

Then the unknown functions F_L and F_R could be written as

$$F_L = \sum_{i=1}^{m} c_{L,i} s_i \,, \quad F_R = \sum_{i=1}^{m} c_{R,i} s_i \,.$$

We expect on physical grounds F_L and F_R to be rather smooth so $r \in N$ could be assumed to be at least 2. This indicates that the Fourier coefficients of the unknown functions

$$\int_0^1 F_L(x^*)\cos(n\pi x^*)dx^* \,, \quad \int_0^1 F_R(x^*)\cos(n\pi x^*)dx^* \,,$$

as well as of the other dependent quantities involved should decay at least as $O(1/n^2)$ or faster. As a consequence, only a small part of the infinite system is expected to be significant for F_L and F_R. Thus, for a particular choice of $m \in N$ only the equations $n = 0, 1, ..., m$ are taken into account. This gives a system of $2(m + 1)$ nonlinear equations for the unknown coefficients

$$\mathbf{c}_L := (c_{L,i})_{i=0}^{m} \,, \quad \mathbf{c}_R := (c_{R,i})_{i=0}^{m} \,,$$

written in short as,

$$\begin{aligned} f(\mathbf{c}_L) &= g_1(\mathbf{c}_L, \mathbf{c}_R), \\ f(\mathbf{c}_R) &= g_2(\mathbf{c}_L, \mathbf{c}_R). \end{aligned} \tag{MN.2}$$

The structure of the system (MN.2) follows from (23) but with (MN.1) added to each equations block. There are two important steps to be considered. The first is the choice of the subspace S_m. We decided to try first perhaps the simplest approach, by choosing the subspace S_m as the space of polynomials $S_m = \mathrm{P}_m$ of degree $\le m$. The numerical results turned out satisfactory. Alternatively, we could always switch to a proper spline space. The second step regards the efficient numerical solution of the system (MN.2). Inspection of the equations (23) reveals that the function f depends linearly on the unknowns. Since the functions g_i are much more complicated, the direct iteration seems to be a cheap shortcut. So, with the starting choice incorporating the conditions (MN.1),

$$c_{L,i}^{(0)} = c_{R,i}^{(0)} = \frac{1}{2(m+1)}, \; i = 1, 2, \ldots, m, \tag{MN.3a}$$

$$c_{L,0}^{(0)} = c_{R,0}^{(0)} = 1 - \frac{1}{2(m+1)} \sum_{i=1}^{m} \frac{1}{i}, \tag{MN.3b}$$

the direct iteration reads,

$$f(\mathbf{c}_L^{(k+1)}) = g_1(\mathbf{c}_L^{(k)}, \mathbf{c}_R^{(k)}),$$

$$f(\mathbf{c}_R^{(k+1)}) = g_2(\mathbf{c}_L^{(k)}, \mathbf{c}_R^{(k)}), \; k = 0, 1, \ldots .$$

This approach was quite satisfactory for some parameter values, but failed to converge for others. Clearly, the map involved in this case ceases to be a contraction. However, the Newton method turned out to be the proper way to solve the system (MN.2). For any consistent data choice and particular m, only several Newton steps were needed. The initial values of the unknowns were again taken as in (MN.3). The Jacobian matrix $J(\mathbf{c}_L, \mathbf{c}_R)$, needed at each Newton step involving the solution of a system of linear equations,

$$J(\mathbf{c}_L^{(k)}, \mathbf{c}_R^{(k)}) = \begin{pmatrix} \Delta\mathbf{c}_L^{(k)} \\ \Delta\mathbf{c}_R^{(k)} \end{pmatrix} = \begin{pmatrix} \boldsymbol{f}(\mathbf{c}_L^{(k)}) - \boldsymbol{g}_1(\mathbf{c}_L^{(k)}, \mathbf{c}_R^{(k)}) \\ \boldsymbol{f}(\mathbf{c}_R^{(k)}) - \boldsymbol{g}_2(\mathbf{c}_L^{(k)}, \mathbf{c}_R^{(k)}) \end{pmatrix},$$

and a correction

$$\begin{pmatrix} \mathbf{c}_L^{(k+1)} \\ \mathbf{c}_R^{(k+1)} \end{pmatrix} = \begin{pmatrix} \mathbf{c}_L^{(k)} \\ \mathbf{c}_R^{(k)} \end{pmatrix} + \begin{pmatrix} \Delta\mathbf{c}_L^{(k)} \\ \Delta\mathbf{c}_R^{(k)} \end{pmatrix}, \quad k = 0, 1, \ldots,$$

admits no close form and has to be computed numerically. It is a simple task to compute all the partial derivatives involved if the three basic terms that depend on the unknown coefficients are determined. A brief outline is as follows. For a given S_m, let $(s_i)_{i=0}^m$ be its basis, and

$$F = \sum_{i=1}^{m} c_i s_i \ , \quad \mathbf{c} := (c_i)_{i=0}^m \ ,$$

stands for F_L and F_R, and

$$\zeta(x) = \int_0^x F(u)du = \sum_{i=0}^{m} c_i \int_0^x s_i(u)du \ .$$

Then

$$\frac{\partial}{\partial c_j} F(x) = s_j(x) \ , \quad \frac{\partial}{\partial c_j} \zeta(x) = \int_0^x s_j(u)du \ , \quad j = 0, 1, \ldots, m.$$

Further,

$$\frac{\partial}{\partial c_j} \int_0^1 F(x)\cos(n\pi x)dx = \int_0^1 s_j(x)\cos(n\pi x)dx \ , \quad j = 0, 1, \ldots, m,$$

which yields all coefficients in both $n = 0$ equations as well as the parts of the elements in J that contribute by the partial derivatives of the function $\boldsymbol{f}$. In order to compute $\partial \boldsymbol{g}_i / \partial c_j$, the following two terms have to be determined,

$$\frac{\partial}{\partial c_j}\int_0^1 \frac{F(x)^{3/2}}{\zeta(x)^{1/4}}\cos(n\pi x)dx = \frac{3}{2}\int_0^1 \frac{F(x)^{1/2}}{\zeta(x)^{1/4}}s_j(x)\cos(n\pi x)dx - \frac{1}{4}\int_0^1 \frac{F(x)^{3/2}}{\zeta(x)^{5/4}}\cos(n\pi x)\int_0^x s_j(u)dudx$$

and

$$\frac{\partial}{\partial c_j}\int_0^1 \frac{\zeta(x)^{3/4}F'(x)}{F(x)^{1/2}}\cos(n\pi x)dx =$$
$$\int_0^1 \frac{2F(x)s_j'(x) - F'(x)s_j(x)}{2F(x)^{3/2}}\zeta(x)^{3/4}\cos(n\pi x)dx - \frac{3}{4}\int_0^1 \frac{F'(x)}{F(x)^{1/2}\zeta(x)^{1/4}}\cos(n\pi x)\int_0^x s_j(u)dudx$$

where the prime indicates the ordinary derivative with respect to x. Since n is rather small, it turned out that the use of the Filon's quadrature rules was not necessary.

8. Nomenclature

$a_{L,R}^{(i)}$	defined by eq. (24)
A	surface area of the wall
$F_{L,R}(x^*)$, $\zeta_{L,R}(x^*)$	defined by eq. (20c)
g	acceleration of gravity
$G = \beta g(T_s - T_{0R})H^3/\nu^2$	Grashof number
$h_{L,R}$	convection transfer coefficients to the left and right of the wall
$J_{L,R}$	defined by eq. (15d)
k	thermal conductivity
L, H	thickness and height of the wall
$\bar{N}u^{(L,R)}$	Nusselt numbers associated with the left- and right-hand surface of the wall
$P = \nu/a$	Prandtl number
$\dot{Q}$, $q = \dot{Q}/A$	heat flow, heat flow density
T_{0L}, $_{0R}$	air temperature far from the wall to the left and right of the wall
$T_{1,2}$	temperature of the left and right wall surface
T_s	characteristic wall surface temperature
$U = k/L$	thermal transmittance
u, v	x- and y-component of the velocity field
$x^* = x/H$, $y^* = y/H$	dimensionless coordinates

Greek symbols

a	thermal diffusivity
β	thermal-expansion coefficient of the air

γ	defined by eq. (15c)
$\zeta_{L,R}(x^*)$	defined by eq. (20c)
η	viscosity
$\kappa_{L,R}$	defined in eq. (15e)
$\nu = \eta/\rho$	kinematic viscosity
ξ	$G_R^{1/4}\, y^*/(4x^*)^{1/4}$
ρ	mass density
$\Phi_{L,R}(\xi)$,	Pohlhausen solution
$\Theta_{L,R}(\xi)$	temperature function associated with $\Phi_{L,R}(\xi)$
$\phi_R(x^*,\xi)$, $\theta_R(x^*,\xi)$	corrections to the Pohlhausen solution introduced in eqs. (5), (6)
ψ	stream function introduced in eq. (5)

Subscripts, superscripts

a	air
L, R	left, right
s	surface
w	wall
*	dimensionless coordinate based on H

9. References

Grimson, J. (1971). *Advanced Fluid Dynamics and Heat Transfer*, McGraw-Hill, Maidenhead, pp. 215-219

Kao, T.T.; G.A. Domoto, G.A. & Elrod, H.G. (1977). Free convection along a nonisothermal vertical flat plate, *Transactions of the ASME*, February 1977, 72-78, ISSN: 0021-9223

Landau, L.D.; Lifshitz, E.M. (1987). *Fluid Mechanics*, ISBN 0-08-033933-6, Pergamon Press, Oxford, pp. 219-220

Miyamoto, M.; Sumikawa, J.; Akiyoshi, T. & Nakamura, T. (1980). Effects of axial heat conduction in a vertical flat plate on free convection heat transfer, *International Journal of Heat and Mass Transfer*, 23, 1545-53, ISSN: 0017-9310

Ostrach, S. (1953). An analysis of laminar free convection flow and heat transfer about a flat plate parallel to the direction of the generating body force, *NACA Report* 1111, 63-79

Pohlhausen, H. (1921). Der Wärmeaustausch zwischen festen Körpern und Flüssigkeiten mit Kleiner Wärmeleitung, *ZAMM* 1, 115-21, ISSN

Pop, I. & Ingham, D.B. (2001). *Convective Heat Transfer*, ISBN 0 08 043878 4, Pergamon Press, Oxford, pp. 181-198

Pozzi, A. & Lupo, M. (1988). The coupling of conduction with laminar natural convection along a flat plate, *International Journal of Heat and Mass Transfer*, 31, 1807-14, ISSN: 0017-9310

Vynnycky, M. & Kimura, S. (1996). Conjugate free convection due to a heated vertical plate, *International Journal of Heat and Mass Transfer*, 39, 1067-80, ISSN: 0017-9310

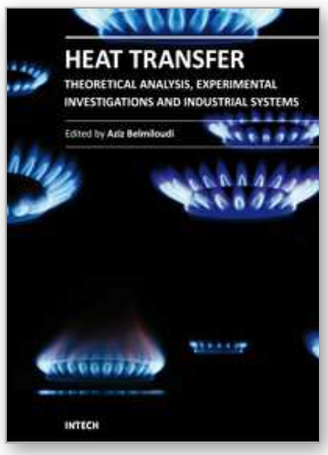

Heat Transfer - Theoretical Analysis, Experimental Investigations and Industrial Systems

Edited by Prof. Aziz Belmiloudi

ISBN 978-953-307-226-5
Hard cover, 654 pages
Publisher InTech
Published online 28, January, 2011
Published in print edition January, 2011

Over the past few decades there has been a prolific increase in research and development in area of heat transfer, heat exchangers and their associated technologies. This book is a collection of current research in the above mentioned areas and discusses experimental, theoretical and calculation approaches and industrial utilizations with modern ideas and methods to study heat transfer for single and multiphase systems. The topics considered include various basic concepts of heat transfer, the fundamental modes of heat transfer (namely conduction, convection and radiation), thermophysical properties, condensation, boiling, freezing, innovative experiments, measurement analysis, theoretical models and simulations, with many real-world problems and important modern applications. The book is divided in four sections : "Heat Transfer in Micro Systems", "Boiling, Freezing and Condensation Heat Transfer", "Heat Transfer and its Assessment", "Heat Transfer Calculations", and each section discusses a wide variety of techniques, methods and applications in accordance with the subjects. The combination of theoretical and experimental investigations with many important practical applications of current interest will make this book of interest to researchers, scientists, engineers and graduate students, who make use of experimental and theoretical investigations, assessment and enhancement techniques in this multidisciplinary field as well as to researchers in mathematical modelling, computer simulations and information sciences, who make use of experimental and theoretical investigations as a means of critical assessment of models and results derived from advanced numerical simulations and improvement of the developed models and numerical methods.

How to reference

In order to correctly reference this scholarly work, feel free to copy and paste the following:

T. Kranjc and J. Peternelj (2011). The Rate of Heat Flow through Non-Isothermal Vertical Flat Plate, Heat Transfer - Theoretical Analysis, Experimental Investigations and Industrial Systems, Prof. Aziz Belmiloudi (Ed.), ISBN: 978-953-307-226-5, InTech, Available from: http://www.intechopen.com/books/heat-transfer-theoretical-analysis-experimental-investigations-and-industrial-systems/the-rate-of-heat-flow-through-non-isothermal-vertical-flat-plate

INTECH
open science | open minds

InTech Europe
University Campus STeP Ri
Slavka Krautzeka 83/A

InTech China
Unit 405, Office Block, Hotel Equatorial Shanghai
No.65, Yan An Road (West), Shanghai, 200040, China

51000 Rijeka, Croatia
Phone: +385 (51) 770 447
Fax: +385 (51) 686 166
www.intechopen.com

中国上海市延安西路65号上海国际贵都大饭店办公楼405单元
Phone: +86-21-62489820
Fax: +86-21-62489821

IntechOpen

IntechOpen